Applied Physics Letters ARTICLE scitation.org/journal/apl

The effect of current density–voltage measurement conditions on the operational stability of hybrid perovskite solar cells

Cite as: Appl. Phys. Lett. **117**, 103503 (2020); doi: 10.1063/5.0023622
Submitted: 30 July 2020 · Accepted: 27 August 2020 ·
Published Online: 10 September 2020

Ganbaatar Tumen-Ulzii,[1,2] Toshinori Matsushima,[2,3,a)] Dino Klotz,[3] and Chihaya Adachi[1,2,3,a)]

AFFILIATIONS

[1]Center for Organic Photonics and Electronics Research (OPERA), Kyushu University, 744 Motooka, Nishi, Fukuoka 819-0395, Japan
[2]Japan Science and Technology Agency (JST), ERATO, Adachi Molecular Exciton Engineering Project, 744 Motooka, Nishi, Fukuoka 819-0395, Japan
[3]International Institute for Carbon-Neutral Energy Research (WPI-I2CNER), Kyushu University, 744 Motooka, Nishi, Fukuoka 819-0395, Japan

[a)]**Authors to whom correspondence should be addressed:** adachi@cstf.kyushu-u.ac.jp or tmatusim@i2cner.kyushu-u.ac.jp

ABSTRACT

Organic–inorganic lead halide perovskites have attracted great attention for use in solar cells, because of their efficient solar power conversion, along with compatibility with simple solution processing. To evaluate the operational stability of perovskite solar cells (PSCs), measurements on their current density–voltage ($J-V$) curves are periodically repeated in most literature studies. However, how the periodic $J-V$ measurements affect the operational stability of PSCs has not been well understood to date. In this study, we found that repeating the $J-V$ measurements, especially applying a voltage higher than the open-circuit voltage of PSCs, under continuous illumination, causes serious ion migration, which lowers the operational stability of PSCs. On the other hand, we observed no decrease in operational stability when the applied voltage is close to or lower than the open-circuit voltage of PSCs during the periodic $J-V$ measurements because of the suppressed ion migration. These findings are important in evaluating the intrinsic operational stability of PSCs.

Organic–inorganic lead halide perovskite solar cells (PSCs) have attracted great attention because of their efficient solar energy conversion.[1–4] By optimizing perovskite fabrication conditions and PSC architectures, the performance of PSCs has dramatically been improved, with the highest certified power conversion efficiency (PCE) having reached 25.2%.[5,6] However, a hysteresis phenomenon is frequently observed when the current density–voltage ($J-V$) curves of PSCs are measured in consecutive forward and reverse scans. One of the origins of this $J-V$ hysteresis is attributed to ion migration.[7,8] Ions and ionic vacancies migrate through the perovskite layer and accumulate at interfaces during the $J-V$ measurements.[9,10] For example, it is known that the accumulation of positive ions at an interface between the electron transport layer and the perovskite layer and the accumulation of negative ions at an interface between the hole transport layer and the perovskite layer lead to nonradiative recombination of holes and electrons,[9–17] thereby inducing the $J-V$ hysteresis.[14,17]

The ion migration also makes the operational stability of PSCs lower; PCEs of PSCs gradually decrease over time under illumination because of the ion migration, which is another serious issue that needs to be solved for future commercialization.[18] This ion-induced PCE decrease is sometimes recoverable by keeping PSCs in the dark condition because the ions return to the original position.[19,20] The operational stability of PSCs has frequently been evaluated by periodically measuring $J-V$ curves with different time intervals. For example, the reported time intervals were 15 (Ref. 4), 30 (Refs. 21 and 22), and 360 (Ref. 23) min. However, the $J-V$ curve measurements are not carried out during solar cell operation implemented in final commercial products. Therefore, it is necessary to clarify the effect of the periodic $J-V$ measurements on the operational stability of PSCs.

To understand how the $J-V$ measurements affect the operational stability clearly, in this study, we measured the $J-V$ curves of PSCs with different voltage scan ranges or time intervals. As a result, we found that applying a voltage higher than the open-circuit voltage (V_{OC}) many times during the stability test accelerates the ion migration and, therefore, causes the PCEs of PSCs to significantly decrease. We were able to suppress the decrease in PCEs by applying a voltage

lower than the V_{OC} or increasing the time intervals of the $J-V$ measurements. Therefore, this work suggests the importance of choosing a suitable $J-V$ measurement condition to know the intrinsic operational stability of PSCs.

The PSC structure used in this study was glass substrate/indium tin oxide (ITO) electrode (100 nm)/tin oxide (SnO_2) electron transport layer (ETL) (~30 nm)/perovskite light absorber (~650 nm)/chemically doped spiro-OMeTAD hole transport layer (HTL) (~150 nm)/Au electrode (100 nm). The composition of the perovskite layer was $Cs_{0.05}(FA_{0.85}MA_{0.15})_{0.95}Pb(I_{0.85}Br_{0.15})_3$ (hereafter abbreviated as CsFAMA). Spiro-OMeTAD, FA, and MA stand for 2,2′,7,7′-tetrakis[*N*,*N*-di(4-methoxyphenyl)amino]-9,9′-spirobifluorene, formamidinium, and methylammonium, respectively. See the supplementary material for details of the PSC fabrication and measurement conditions.

Figure 1(a) shows the $J-V$ characteristics of PSCs measured three times subsequently with a voltage bias range from 1.2 to –0.1 V under the AM 1.5 G (1 sun) condition. Table S1 summarizes the short-circuit current density (J_{SC}), V_{OC}, fill factor (FF), and PCE values extracted from Fig. 1(a). The first $J-V$ measurement led to a PCE value of 17.5% as indicated by the red line of Fig. 1(a). The PCEs decreased to 14.73% and 13.17% when the $J-V$ measurements were further repeated [the blue and green lines in Fig. 1(a)]. As we will discuss later, applying a voltage higher than the V_{OC} (~1.06 V) to PSCs is one source of the PSC performance degradation. After the $J-V$ measurements three times under the illumination, PSCs were placed in the dark, and their performance was recovered with time [the orange and black lines in Fig. 1(a)]. Nearly 100% recovery was obtained after 3 h of storage in the dark. A similar reversible behavior of PSC performance was observed in a previous report,[19] which was attributed to the ion migration effect.

The ion migration is unlikely in the dark because the activation energy for the ion migration is very high in the dark compared with under the illumination.[24] To check if the ion migration occurs in our PSCs in the dark, we carried out a couple of $J-V$ measurements as follows. A $J-V$ curve was first measured under the illumination as indicated by a red line of Fig. 1(b) and Table S2. After PSCs were kept in the dark for at least 3 h, dark $J-V$ curves were measured three times as shown by the black, orange, and pink dashed lines of Fig. 1(b) and Table S2. Right after these dark measurements, a $J-V$ curve was measured under the illumination [the blue line in Fig. 1(b) and Table S2]. The PCEs were almost similar before and after the dark $J-V$ measurements three-times, indicating the negligible effect of the dark $J-V$ measurements on the ion migration.

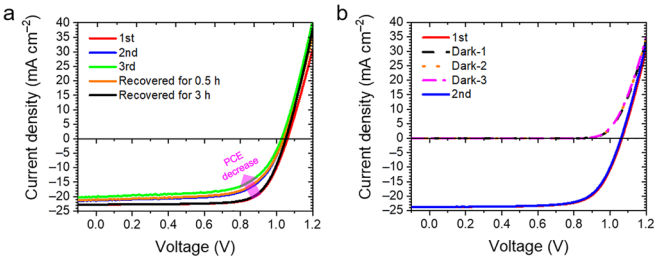

FIG. 1. (a) and (b) $J-V$ curves of PSCs. (a) We subsequently measured the $J-V$ curves three times under the illumination. The red, blue, and green curves correspond to the $J-V$ curves measured with first, second, and third scans, respectively. After the aforementioned three-times $J-V$ measurements, we placed PSCs in the dark for 0.5 or 3 h. Then, we measured $J-V$ curves again under the illumination. The orange and black curves correspond to the $J-V$ curves measured after placing PSCs in the dark for 0.5 and 3 h, respectively. (b) We first measured a $J-V$ curve under the illumination (the red curve). After we placed PSCs in the dark for 3 h, we measured $J-V$ curves three times under the dark (the black, orange, and pink curves). Just after the dark measurements, we measured a $J-V$ curve under the illumination (the blue curve). The $J-V$ measurement condition used here was a voltage scan from 1.2 V (above the V_{OC}) to −0.1 V.

To obtain insight into the observed PCE decrease shown in Fig. 1(a), we repeated $J-V$ measurements on fresh PSCs three times with different voltage scan ranges under the illumination (Fig. 2). The voltage scan ranges used here were from 1.06 (close to the V_{OC}) to –0.1 V and from 1.0 (below the V_{OC}) to –0.1 V. Interestingly, compared with the previous voltage scan range from 1.2 V (above the V_{OC}) to –0.1 V, these voltage scan ranges did not decrease the PSC performance. This indicates that applying a voltage higher than the V_{OC} to PSCs induces the PSC performance degradation.

Based on the aforementioned results, we illustrate the ion migration dynamics when a voltage above the V_{OC}, close to the V_{OC}, or below the V_{OC} is applied to PSCs (Fig. 3). When the applied voltage is higher than the V_{OC}, the ion migration occurs under the illumination with a driving force of the electric field; positively charged ions move to the SnO_2 side and negatively charged ions move to the spiro-OMeTAD side as shown in Fig. 3(a). Since these ions accumulating at the interfaces impede the charge extraction to the electrodes,[14,17] it is reasonable that PCEs of PSCs decrease. In contrast, there is no significant ion migration occurring in PSCs when the applied voltage is close to or lower than the V_{OC}, because the electric field gradient is flat [Fig. 3(b)] or its direction is opposite [Fig. 3(c)].

Next, we checked how $J-V$ measurements affect the operational stability of PSCs under the illumination. For this purpose, we measured $J-V$ curves every 10 min with the three different voltage scan ranges used earlier. In between $J-V$ scans, the PSCs were put at a maximum power point (MPP) condition under the continuous illumination from a white LED with a light intensity of 100 mW cm^{-2}. As shown in Fig. 4(a), it was clear that the PSC degradation happened only when a voltage above the V_{OC} was applied. This is consistent with the earlier discussion on the ion migration caused by the application of the high voltage. Furthermore, this PSC degradation was ~100% recoverable by keeping the PSCs in the dark for 3 h, which is similar to the $J-V$ curves returning to the original position in the dark as we discussed earlier.

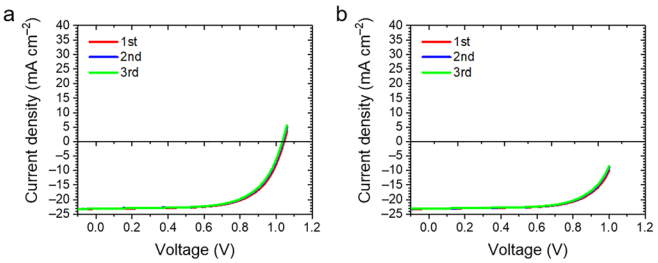

FIG. 2. $J-V$ curves of PSCs measured three times with voltage scan ranges (a) from 1.06 V (close to the V_{OC}) to –0.1 V and (b) from 1.0 V (below the V_{OC}) to –0.1 V under the illumination.

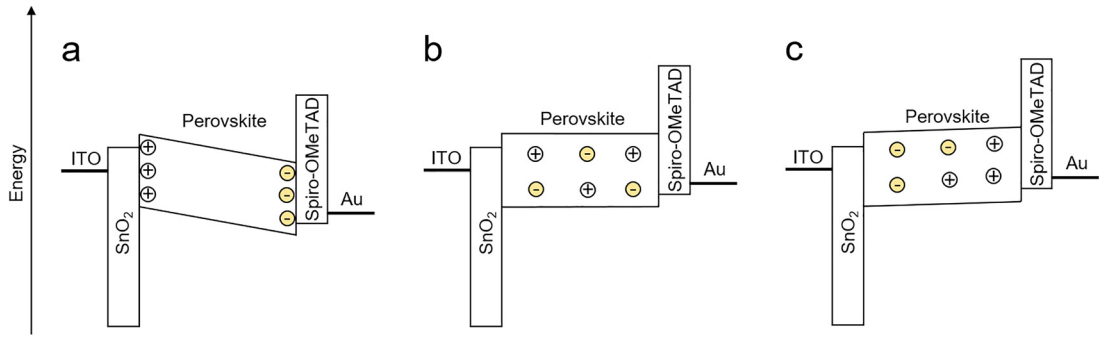

FIG. 3. Energy-level diagrams of PSCs with an applied voltage, which is (a) higher than, (b) close to, or (c) lower than the V_{OC}.

Before and after the operational stability measurement for 1440 min (24 h), we removed the Au and spiro-OMeTAD layers from PSCs using a method we previously reported (Ref. 25) and measured the x-ray diffraction (XRD) patterns and top-view scanning electron microscope (SEM) images of the CsFAMA perovskite layer surfaces. As results, we observed no appreciable degradation of the CsFAMA perovskite layers after the operation (Fig. S1).

Next, we repeated the operational stability measurements under the illumination for ∼24 h and under dark storage for ∼3 h (Fig. S2). The ∼100% PCE recovery was difficult to obtain after the third dark storage, which could be related to destabilization of ions in the perovskite lattice, leading to permanent degradation.[19]

Furthermore, we tested if a similar PCE recovery behavior can be seen from other methylammonium lead triiodide ($MAPbI_3$)-based PSCs. However, no PCE recovery was observed in $MAPbI_3$-based PSCs (Fig. S3).

We conducted an additional stability test with the voltage scan range from 1.2 V (over the V_{OC}) to −0.1 V and different time intervals of 5, 10, 15, 20, 60, and 1440 (only two times at the start and end points) min for $J-V$ measurements. The operational stability decreased as the measurement time intervals were decreased [Fig. 4(b)]. When the intervals were 20 min or longer, the PSC degradation was not observed. This indicates that the measurement interval of at least 20 min is required to cause the ions to return in the CsFAMA-based PSCs we used in this study. To check reproducibility, we carried out the same stability test on nine individual PSCs with different two intervals of 10 and 1440 min. We obtained the similar degradation behaviors (Fig. S4). Furthermore, we tested the stability of PSCs at an elevated temperature of 40 °C by measuring the $J-V$ curves twice at the start and end points with a long interval of 1440 min. Although the negligible change of the PCE was observed at room temperature (∼25 °C), the PCE significantly decreased at 40 °C (Fig. S5), probably because of the ion migration being accelerated at the high temperature.

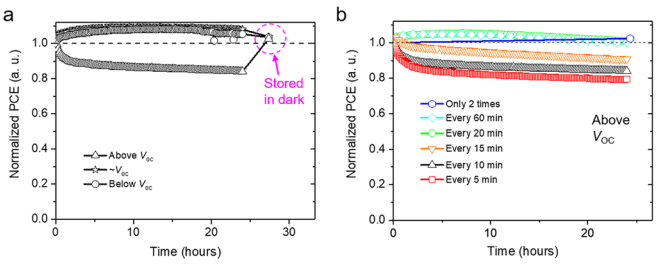

FIG. 4. Evolution of PCEs when PSCs were operated under the continuous illumination at the MPP condition. The triangle, star, and circle symbols in (a) indicate the PCEs calculated from $J-V$ curves measured with the voltage scan ranges from 1.2 V (above the V_{OC}) to −0.1 V, from 1.06 V (close to the V_{OC}) to −0.1 V, and from 1.0 V (below the V_{OC}) to −0.1 V, respectively. The measurement time interval was 10 min. (b) indicates the evolution of PCEs calculated from $J-V$ curves measured with the voltage scan range from 1.2 V (above the V_{OC}) to −0.1 V and the different time intervals of 5 (red), 10 (black), 15 (orange), 20 (green), 60 (light blue), and 1440 (blue; the measurements at the initial and end points only) min, respectively. The black triangle symbols in (b) are taken from (a) for comparison.

In this Letter, we studied the effect of the $J-V$ measurements on the operational stability of PSCs during the continuous illumination. We found that repeating $J-V$ curve measurements decreased the operational stability of PSCs, because of the ion migration. Especially, applying a voltage higher than the V_{OC} markedly accelerated the ion migration. Since typical solar cell products are usually operated below V_{OC}, this type of device degradation associated with the ion migration would be negligible in products. Thus, we need to pay attention to a stability measurement condition to know the intrinsic degradation behaviors of PSCs.

See the supplementary material for the experimental details, SEM and XRD results, operational stability of PSCs under operation with other conditions, and summary of solar cell parameters.

This work was supported by the Japan Science and Technology Agency (JST), ERATO, Adachi Molecular Exciton Engineering Project (JST ERATO Grant No. JPMJER1305); the International Institute for Carbon-Neutral Energy Research (No. WPI-I2CNER) sponsored by the Ministry of Education, Culture, Sports, Science and Technology (MEXT) of Japan; JSPS KAKENHI (Grant Nos. JP15K14149, JP16H04192, and 20H02817); The Canon Foundation; and The Samco Foundation.

DATA AVAILABILITY

The data that support the findings of this study are available from the corresponding author upon reasonable request.

REFERENCES

[1]A. Kojima, K. Teshima, Y. Shirai, and T. Miyasaka, J. Am. Chem. Soc. **131**, 6050 (2009).
[2]H. S. Kim, C. R. Lee, J. H. Im, K. B. Lee, T. Moehl, A. Marchioro, S. J. Moon, R. Humphry-Baker, J. H. Yum, J. E. Moser, M. Grätzel, and N. G. Park, Sci. Rep. **2**, 591 (2012).
[3]N. J. Jeon, J. H. Noh, W. S. Yang, Y. C. Kim, S. Ryu, J. Seo, and S. Il Seok, Nature **517**, 476 (2015).
[4]M. Saliba, T. Matsui, J. Y. Seo, K. Domanski, J. P. Correa-Baena, M. K. Nazeeruddin, S. M. Zakeeruddin, W. Tress, A. Abate, A. Hagfeldt, and M. Grätzel, Energy Environ. Sci. **9**, 1989 (2016).
[5]National Renewable Energy Laboratory, see https://www.nrel.gov/pv/assets/pdfs/best-research-cell-efficiencies.20200406.pdf for "Best Research-Cell Efficiency Chart."
[6]Q. Jiang, Y. Zhao, X. Zhang, X. Yang, Y. Chen, Z. Chu, Q. Ye, X. Li, Z. Yin, and J. You, Nat. Photonics **13**, 500 (2019).
[7]S.-G. Kim, C. Li, A. Guerrero, J.-M. Yang, Y. Zhong, J. Bisquert, S. Huettner, and N.-G. Park, J. Mater. Chem. A **7**, 18807 (2019).
[8]W. Tress, J. Phys. Chem. Lett. **8**, 3106 (2017).
[9]R. A. Belisle, W. H. Nguyen, A. R. Bowring, P. Calado, X. Li, S. J. C. Irvine, M. D. McGehee, P. R. F. Barnes, and B. C. O'Regan, Energy Environ. Sci. **10**, 192 (2017).
[10]F. Wu, B. Bahrami, K. Chen, S. Mabrouk, R. Pathak, Y. Tong, X. Li, T. Zhang, R. Jian, and Q. Qiao, ACS Appl. Mater. Interfaces **10**, 25604 (2018).
[11]S. A. L. Weber, I. M. Hermes, S. H. Turren-Cruz, C. Gort, V. W. Bergmann, L. Gilson, A. Hagfeldt, M. Grätzel, W. Tress, and R. Berger, Energy Environ. Sci. **11**, 2404 (2018).
[12]J. Carrillo, A. Guerrero, S. Rahimnejad, O. Almora, I. Zarazua, E. Mas-Marza, J. Bisquert, and G. Garcia-Belmonte, Adv. Energy Mater. **6**, 1502246 (2016).
[13]T. Zhang, S. H. Cheung, X. Meng, L. Zhu, Y. Bai, C. H. Y. Ho, S. Xiao, Q. Xue, S. K. So, and S. Yang, J. Phys. Chem. Lett. **8**, 5069 (2017).
[14]J. P. Correa-Baena, S. H. Turren-Cruz, W. Tress, A. Hagfeldt, C. Aranda, L. Shooshtari, J. Bisquert, and A. Guerrero, ACS Energy Lett. **2**, 681 (2017).
[15]T. Zhang, H. Chen, Y. Bai, S. Xiao, L. Zhu, C. Hu, Q. Xue, and S. Yang, Nano Energy **26**, 620 (2016).
[16]Y. Deng, Z. Xiao, and J. Huang, Adv. Energy Mater. **5**, 1500721 (2015).
[17]R. Gottesman, P. Lopez-Varo, L. Gouda, J. A. Jimenez-Tejada, J. Hu, S. Tirosh, A. Zaban, and J. Bisquert, Chem **1**, 776 (2016).
[18]L. Meng, J. You, and Y. Yang, Nat. Commun. **9**, 5265 (2018).
[19]K. Domanski, B. Roose, T. Matsui, M. Saliba, S. H. Turren-Cruz, J. P. Correa-Baena, C. R. Carmona, G. Richardson, J. M. Foster, F. De Angelis, J. M. Ball, A. Petrozza, N. Mine, M. K. Nazeeruddin, W. Tress, M. Grätzel, U. Steiner, A. Hagfeldt, and A. Abate, Energy Environ. Sci. **10**, 604 (2017).
[20]M. V. Khenkin, K. M. Anoop, I. Visoly-Fisher, S. Kolusheva, Y. Galagan, F. Di Giacomo, O. Vukovic, B. R. Patil, G. Sherafatipour, V. Turkovic, H. G. Rubahn, M. Madsen, A. V. Mazanik, and E. A. Katz, ACS Appl. Energy Mater. **1**, 799 (2018).
[21]M. Saliba, T. Matsui, K. Domanski, J. Y. Seo, A. Ummadisingu, S. M. Zakeeruddin, J. P. Correa-Baena, W. R. Tress, A. Abate, A. Hagfeldt, and M. Grätzel, Science **354**, 206 (2016).
[22]J. A. Christians, P. Schulz, J. S. Tinkham, T. H. Schloemer, S. P. Harvey, B. J. Tremolet De Villers, A. Sellinger, J. J. Berry, and J. M. Luther, Nat. Energy **3**, 68 (2018).
[23]S. Yang, S. Chen, E. Mosconi, Y. Fang, X. Xiao, C. Wang, Y. Zhou, Z. Yu, J. Zhao, Y. Gao, F. De Angelis, and J. Huang, Science **365**, 473 (2019).
[24]J. Xing, Q. Wang, Q. Dong, Y. Yuan, Y. Fang, and J. Huang, Phys. Chem. Chem. Phys. **18**, 30484 (2016).
[25]G. Tumen-Ulzii, C. Qin, D. Klotz, M. R. Leyden, P. Wang, M. Auffray, T. Fujihara, T. Matsushima, J.-W. Lee, S.-J. Lee, Y. Yang, and C. Adachi, Adv. Mater. **32**, 1905035 (2020).

Supporting information for

The effect of current density–voltage measurement conditions on the operational stability of hybrid perovskite solar cells

Ganbaatar Tumen-Ulzii[1,2], *Toshinori Matsushima*[2,3,a)], *Dino Klotz*[3], *and Chihaya Adachi*[1,2,3,a)]

[1]Center for Organic Photonics and Electronics Research (OPERA), Kyushu University, 744 Motooka, Nishi, Fukuoka 819-0395, Japan

[2]Japan Science and Technology Agency (JST), ERATO, Adachi Molecular Exciton Engineering Project, 744 Motooka, Nishi, Fukuoka 819-0395, Japan

[3]International Institute for Carbon-Neutral Energy Research (WPI-I^{2}CNER), Kyushu University, 744 Motooka, Nishi, Fukuoka 819-0395, Japan

[a)]Author to whom correspondence should be addressed: adachi@cstf.kyushu-u.ac.jp or tmatusim@i2cner.kyushu-u.ac.jp

Methods

Materials. A SnO_2 colloidal precursor solution [tin(IV) oxide, 15% in H_2O colloidal dispersion] was purchased from Alfa Aesar. All precursor materials for the perovskite fabrication, such as cesium iodide (CsI), formamidinium iodide (FAI), methylammonium bromide (MABr), methylammonium iodide (MAI), lead iodide (PbI_2) and lead bromide ($PbBr_2$), were purchased from Tokyo Chemical Industry. Spiro-OMeTAD was purchased from Merck. The organic solvents, such as chlorobenzene, *N,N*-Dimethylformamide (DMF) and dimethyl sulfoxide (DMSO), and chemical dopants for spiro-OMeTAD, such as lithium bis(trifluoromethanesulfonyl)imide (LiTFSI), 4-tert-butylpyridine (4-tBP) and tris(2-(1H-pyrazol-1-yl)-4-*tert*-butylpyridine)cobalt(III) tri[bis(trifluoromethane)sulfonimide] (FK-209), were purchased from Sigma-Aldrich. The above purchased materials were used without further purification.

Device fabrication. Glass substrates coated with a pre-patterned ITO layer with a thickness of 100 nm (Atsugi Micro) and a sheet resistance of 10 Ω $sq.^{-1}$ were cleaned sequentially by ultrasonicating in a detergent aqueous solution, pure water, acetone, and isopropanol for 10 min each, followed by subjecting to UV-ozone treatment for 15 min. A SnO_2 layer was deposited on the ITO substrates through spin-coating at 3,000 rpm for 30 sec using a SnO_2 colloidal solution, which was diluted to ~2.67% in water. The spin-coated SnO_2 layer was annealed at 150 °C for 30 min in ambient air, and then treated by UV-ozone for 15 min. For the perovskite layer fabrication, a precursor solution was prepared by mixing FAI (1.10 M), PbI_2 (1.16 M), MABr (0.2 M) and $PbBr_2$ (0.2 M) in anhydrous DMF/DMSO (4:1 by vol). Additionally, 0.08 M CsI was added to the precursor solution from a stock solution of 1.5 M CsI in DMSO. The precursor solution was stirred at 70 °C for 3 hours and then filtered using a 0.2 μm polytetrafluoroethylene (PTFE) filter before use. A perovskite layer was spin-coated on the SnO_2 layer using the precursor solution at 1,000 rpm for 10 sec and then at 6,000 rpm for 30 sec. Before the end of the spin coating procedure (10 sec before), 120 μl of chlorobenzene was dropped onto the spinning substrate. Subsequently, the perovskite layer was annealed at 100 °C for 30 min. A spiro-OMeTAD layer was deposited on top of the perovskite layer by spin-coating at 4000 rpm for 30 sec from a solution of 36.5 mg of spiro-OMeTAD in

0.5 ml of chlorobenzene. Additionally, this solution was doped with 15 µl of 4-tBP, 9 µl of a LiTFSI stock solution (520 mg ml^{-1} in acetonitrile) and 14.5 µl of an FK209 stock solution (300 mg ml^{-1} in acetonitrile). Finally, a 100-nm-thick gold electrode was thermally deposited to complete the devices. All the devices were encapsulated using a glass lid and UV-cured sealant in a nitrogen-filled glove box.

The $MAPbI_3$-based PSC architecture was glass substrate/ITO/SnO_2/$MAPbI_3$/spiro-OMeTAD/Au. A $MAPbI_3$ perovskite layer was spin-coated on the SnO_2 layer using a 1 M stoichiometric precursor solution (MAI:PbI_2 = 1:1 by mol) at 4,000 rpm for 30 sec. After starting the spin coating procedure (5 sec), 200 µl of chlorobenzene was dropped onto the spinning substrate. Subsequently, the perovskite layer was annealed at 100 °C for 30 min. We used the same conditions described earlier for the fabrication of the other layers.

Characterization. *J–V* curve measurements were performed on PSCs using a computer-controlled Keithley 2400 sourcemeter unit under the simulated AM1.5G solar illumination from a Xe lamp-based solar simulator (SRO-25 GD, Bunko-keiki) with a scan rate of 0.2 V s^{-1}. The active area of the PSCs was defined to be 3.24 mm^2 (1.8 × 1.8 mm^2) using a black shadow mask. The original device area defined by the overlap of the ITO and Au electrodes was 4 mm^2. The lamp power was carefully calibrated at 100 mW cm^{-2} (1 sun) using a crystalline Si reference cell with an amorphous Si optical filter (Bunko-keiki), which was certificated by the National Institute of Advanced Industrial Science and Technology of Japan.

Device lifetime measurements. White light from a light-emitting diode array with an intensity of 100 mW cm^{-2} was continuously illuminated on the PSCs at room temperature. The *J–V* curves were periodically measured with different voltage scan ranges and time intervals using a lifetime measurement system (System Engineers). In between *J–V* scans, the PSCs were kept at the MPP under a load from a 1 kΩ resistor.

Perovskite film analysis. SEM images of perovskite films were taken using a JEOL JCM-5700 system at an acceleration voltage of 5 kV with magnifications of × 30,000. XRD patterns of perovskite films were evaluated using out-of-plane symmetric 2θ/θ

scans on a diffractometer (Rigaku, SmartLab) equipped with Cu rotating anode [λ = 1.542 Å (CuKα)] and a Göbel mirror.

Supplementary figures.

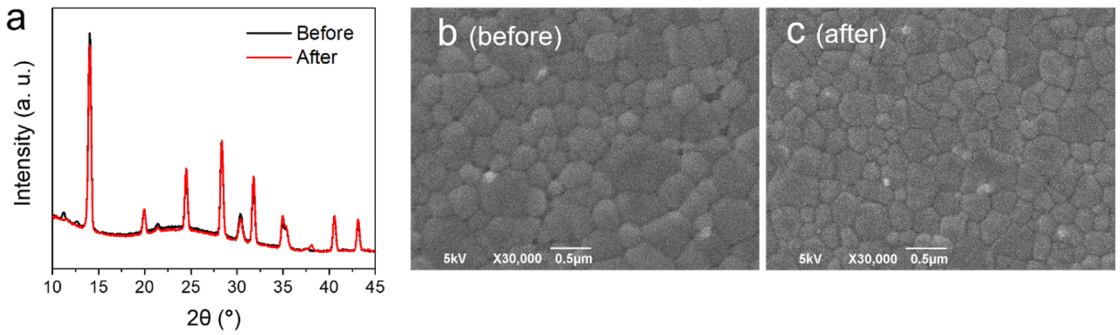

Figure S1. XRD patterns and top-view SEM images of perovskite layers before and after ~24 hours of the stability evaluation under the illumination. These XRD patterns and top-view SEM images were measured after removing the Au and spiro-OMeTAD layers from PSCs.

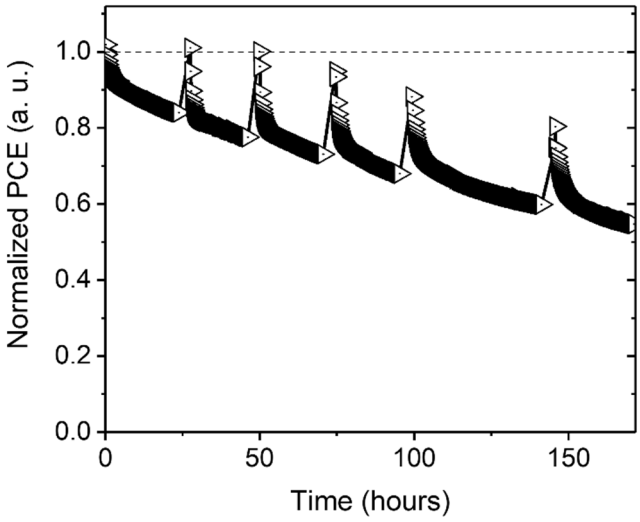

Figure S2. PCE recovery behavior over time. PSCs were operated under the continuous illumination at the MPP condition. The time interval between the *J*–*V* measurements was 10 min, and the voltage bias range was from 1.2 to –0.1 V. To check the PCE recovery, PSCs were periodically stored in the dark for ~3 hours. The PCE jumps in the figure correspond to each dark storage.

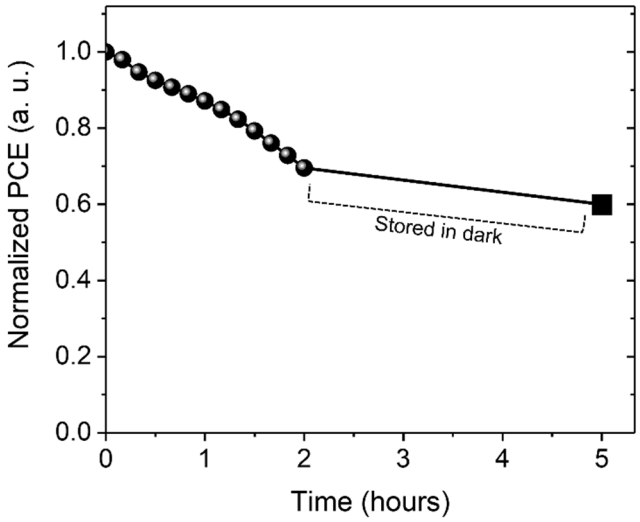

Figure S3. Evolution of PCEs of $MAPbI_3$-based PSCs, which were operated under the continuous illumination at the MPP condition by measuring *J*–*V* curves with a voltage scan range from 1.2 (above the V_{OC}) to −0.1 V. After the storage of PSCs in the dark, PCEs were not recovered.

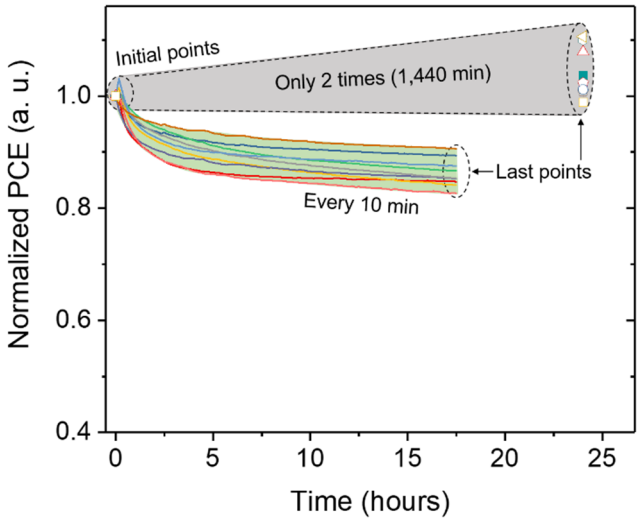

Figure S4. Evolution of PCEs of PSCs under the continuous illumination at the MPP condition. The different two time intervals of 10 and 1,440 min were used to obtain this data. The voltage scan range was from 1.2 (above the V_{OC}) to −0.1 V.

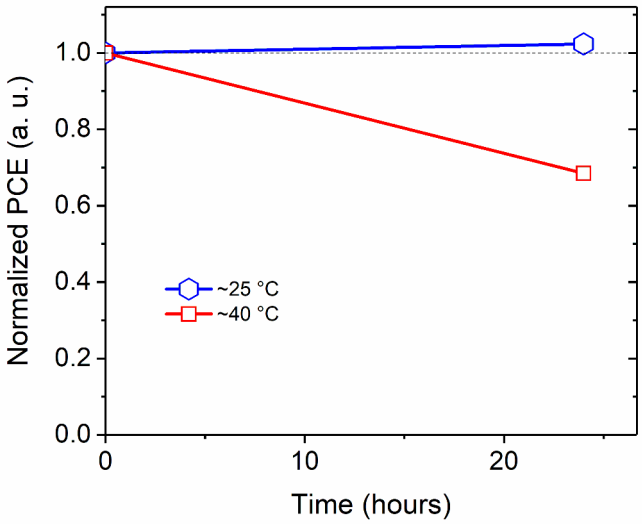

Figure S5. Evolution of PCEs at 40 °C (red) and 25 °C (blue). PCEs were calculated from J−V curves with the voltage scan range from 1.2 (above the V_{OC}) to −0.1 V. The blue plot is taken from Fig. 4b.

Supplementary tables.

Table S1. J_{SC}, V_{OC}, FF, and PCE values extracted from Fig. 1a.

Measurement condition	J_{SC} (mA cm^{-2})	V_{OC} (V)	FF	PCE (%)
1st scan under illumination	–22.78	1.06	0.73	17.75
2nd scan under illumination	–21.29	1.04	0.65	14.73
3rd scan under illumination	–20.11	1.03	0.62	13.17
4th scan under illumination after storage in dark for 0.5 hours	–21.13	1.04	0.63	14.35
5th scan under illumination after storage in dark for 3.0 hours	–22.81	1.05	0.73	17.52

Table S2. J_{SC}, V_{OC}, FF, and PCE values extracted from Fig. 1b.

Measurement condition	J_{SC} (mA cm^{-2})	V_{OC} (V)	FF	PCE (%)
1st scan under illumination	–23.80	1.07	0.72	18.23
2nd scan under dark after storage in dark for 3 hours	N/A	N/A	N/A	N/A
3rd scan under dark	N/A	N/A	N/A	N/A
4th scan under dark	N/A	N/A	N/A	N/A
5th scan under illumination	–23.78	1.06	0.72	17.97